Available online at www.sciencedirect.com

ScienceDirect

Current Opinion in Biomedical Engineering

A suite of neurophotonic tools to underpin the contribution of internal brain states in fMRI

Philipp Mächler[1,2], Thomas Broggini[2], Celine Mateo[2], Martin Thunemann[1], Natalie Fomin-Thunemann[1], Patrick R. Doran[1], Ikbal Sencan[3], Kivilcim Kilic[1], Michèle Desjardins[4], Hana Uhlirova[5], Mohammad A. Yaseen[3,6], David A. Boas[1], Andreas A. Linninger[7], Massimo Vergassola[2,8], Xin Yu[3], Laura D. Lewis[1], Jonathan R. Polimeni[3], Bruce R. Rosen[3], Sava Sakadžić[3], Richard B. Buxton[9], Martin Lauritzen[10,11], David Kleinfeld[2,12] and Anna Devor[1,3]

Abstract

Recent developments in optical microscopy, applicable for large-scale and longitudinal imaging of cortical activity in behaving animals, open unprecedented opportunities to gain a deeper understanding of neurovascular and neurometabolic coupling during different brain states. Future studies will leverage these tools to deliver foundational knowledge about brain state-dependent regulation of cerebral blood flow and metabolism, as well as regulation as a function of brain maturation and aging. This knowledge is of critical importance to interpret hemodynamic signals observed with functional magnetic resonance imaging (fMRI).

Addresses

[1] Department of Biomedical Engineering, Boston University, Boston, MA, 02215, USA
[2] Department of Physics, University of California San Diego, La Jolla, CA, 92093, USA
[3] Athinoula A. Martinos Center for Biomedical Imaging, Department of Radiology, Harvard Medical School, Massachusetts General Hospital, Charlestown, MA, 02129, USA
[4] Département de Physique, de Génie Physique et D'Optique, Université Laval, Québec, QC, G1V 0A6, Canada
[5] Institute of Scientific Instruments of the Czech Academy of Science, Brno, Czech Republic
[6] Department of Bioengineering, Northeastern University, Boston, MA, 02115, USA
[7] Department of Bioengineering, University of Illinois at Chicago, Chicago, IL, 60607, USA
[8] Département de Physique de L'Ecole Normale Supérieure, 75005, Paris, France
[9] Department of Radiology, University of California San Diego, La Jolla, CA, 92037, USA
[10] Department of Neuroscience and Pharmacology, University of Copenhagen, Copenhagen, N 2200, Denmark
[11] Department of Clinical Neurophysiology, Glostrup Hospital, Glostrup, 2600, Denmark
[12] Section on Neurobiology, University of California San Diego, La Jolla, CA, 92093, USA

Corresponding author: Devor, Anna (adevor@bu.edu)

Current Opinion in Biomedical Engineering 2021, **18:**100273

This review comes from a themed issue on **Neural Engineering: Brain-computer interface and functional brain imaging**

Edited by **Bin He and Zhongming Liu**

Received 22 November 2020, revised 19 January 2021, accepted 29 January 2021

Available online xxx

https://doi.org/10.1016/j.cobme.2021.100273

Keywords

Neuromodulation, Optical imaging, Hemodynamic, $CMRO_2$, Glycolysis.

Introduction

Advancing our ability to accurately infer microscopic details underlying noninvasive imaging signals requires direct measurement and manipulation of concrete, cellular level physiological parameters. These measurements are only available in model organisms such as mice. Recent progress in large-scale microscopic imaging technology and the development of genetically encoded optical probes have enabled chronic imaging in awake behaving mice. This opens the door for longitudinal studies of brain neuronal, vascular, and metabolic function across specific behavioral states that differ in the processing capacity of cortical neuronal circuits. Here, we highlight several novel neurophotonics tools in the context of specific neuroscience problems that have moved within reach of the greater research community.

Spontaneous large-scale cortical activity and physiological underpinning of resting-state fMRI

The puzzling phenomenon of spontaneous large-scale cortical activity

Spontaneous large-scale neuronal activity, and activity that far extends beyond the boundaries of receptive fields from punctate stimulation, is a long-recognized aspect of neuronal dynamics that has received renewed attention in light of its potential impact on neurocomputation [1–3]. While large-scale patterns of brain activity have been described since the earliest days of electrophysiological measurements with awake animals, a striking advance occurred with the advent of Blood Oxygenation Level-Dependent (BOLD) functional Magnetic Resonance Imaging (fMRI) in resting human subjects close to two decades ago (reviewed in Ref. [4]). These fMRI studies revealed large-scale, coherent fluctuations of the fMRI signal that resemble the known pattern of functionally engaged cortical regions [5–8]. The BOLD signal reflects hemodynamics and O_2 metabolism rather than neuronal activity *per se* [9,10]; therefore, the possibility that these spatial patterns of temporally coordinated hemodynamic fluctuations, dubbed 'resting-state' networks, reflect spontaneous neuronal activity was initially met with skepticism; however, today, a large body of experimental evidence demonstrates that these signals are significantly, albeit incompletely driven by neuronal activity in rodents, nonhuman primates, and humans [11–26].

In mice, recent technological advances now allow chronic imaging of the entire dorsal part of the cortex. These advances include large field-of-view or multi-region two-photon microscopes [27–30], mesoscopic single-photon imagers [13,31], and novel techniques to produce large cranial windows [32,33]. Combined with genetically encoded calcium (Ca^{2+}) indicators of neuronal activity [34], which record a trace of neuronal spiking, these tools obtain a glimpse of the large-scale spontaneous neuronal activity that contributes to resting-state hemodynamic fluctuations [11,13–16].

Large-scale cortical neuronal activity and ascending neuromodulation

One possibility for the generation of spontaneous large-scale neuronal activity is that the dynamics reflect a continuous 'handshaking' of synaptically connected brain regions [4]; however, some of the observed co-varying areas are not directly anatomically connected, such as the primary visual cortex across the two hemispheres. An alternative explanation for this neuronal activity is common inputs [35], which include ascending neuromodulation [4,36–38], such as cholinergic projections from the basal forebrain [39], adrenergic projections from the locus coeruleus [40,41], dopaminergic projections from the ventral tegmental area and the substantia nigra [42], and serotonergic projections from the raphe nuclei [43]. These neuromodulatory systems work in parallel to generate internal brain states that differ in the attentional capability and processing capacity of cortical circuits [44,45].

Although state-dependent neurovascular coupling remains largely unexplored, arousal states, including rapid eye movement (REM) and nonrapid eye movement (NREM) sleep, have been shown to strongly modulate hemodynamic signals in mice that naturally fall asleep during imaging [46]. This finding is in agreement with the known vasoactive role of neuromodulatory transmitters that can act on vascular receptors [47] in addition to the modulating activity of neuronal circuits. Pharmacological activation of these receptors, including those selectively expressed in microvessels, was demonstrated to affect cerebral blood flow (CBF) and the BOLD signal [48].

Electrophysiologically, brain states of attention, arousal, and vigilance are manifested by 'desynchronized' cortical local field potential (LFP), where the power of low-frequency rhythmicity (<30 Hz) decrements and the power of high frequencies or γ-band rhythmicity (∼30–90 Hz) increases [49]. The power of the γ-band oscillations cofluctuates in brain regions with a shared function. In resting mice, the state of arousal fluctuates continuously on the scale of tens of seconds; this supports the idea that ultraslow (∼0.1 Hz) fluctuations in the γ-band power may be reflecting internal brain state dynamics [50].

Recently, using optical imaging methods, Mateo et al. [12] have demonstrated in an awake mouse study that these ultra-slow frequency fluctuations in the γ-band power, that is, variations around 0.1 Hz, will entrain the dynamics of vasomotion in pial arterioles. This coupled the slowly varying amplitude of the ongoing γ-band rhythm to the resting-state fMRI signal [12] (Figure 1). This finding is apparently at odds with a recent study in awake monkeys showing that pharmacological inactivation of the basal forebrain, a center for cholinergic innervation, selectively diminished only spatially very broad hemodynamic correlations within the affected hemisphere, while finer scale correlations remained [39]; however, the effect of inactivation depended on the level of arousal and suggests possible engagement of other neuromodulation systems, including intrinsic cholinergic neurons in the cortex [51], to compensate for cholinergic 'denervation'.

The activity of specific neuromodulatory afferents in the cerebral cortex can now be directly measured, in real time in animals, with sensitive optical probes for the respective neurotransmitters [52], including acetylcholine [53,54], norepinephrine [55], dopamine [55,56], and serotonin [57]. This formidable advance in molecular engineering offers direct sensing of these neurotransmitters' release in the cerebral cortex. With these tools, one can ask which of the respective

Figure 1

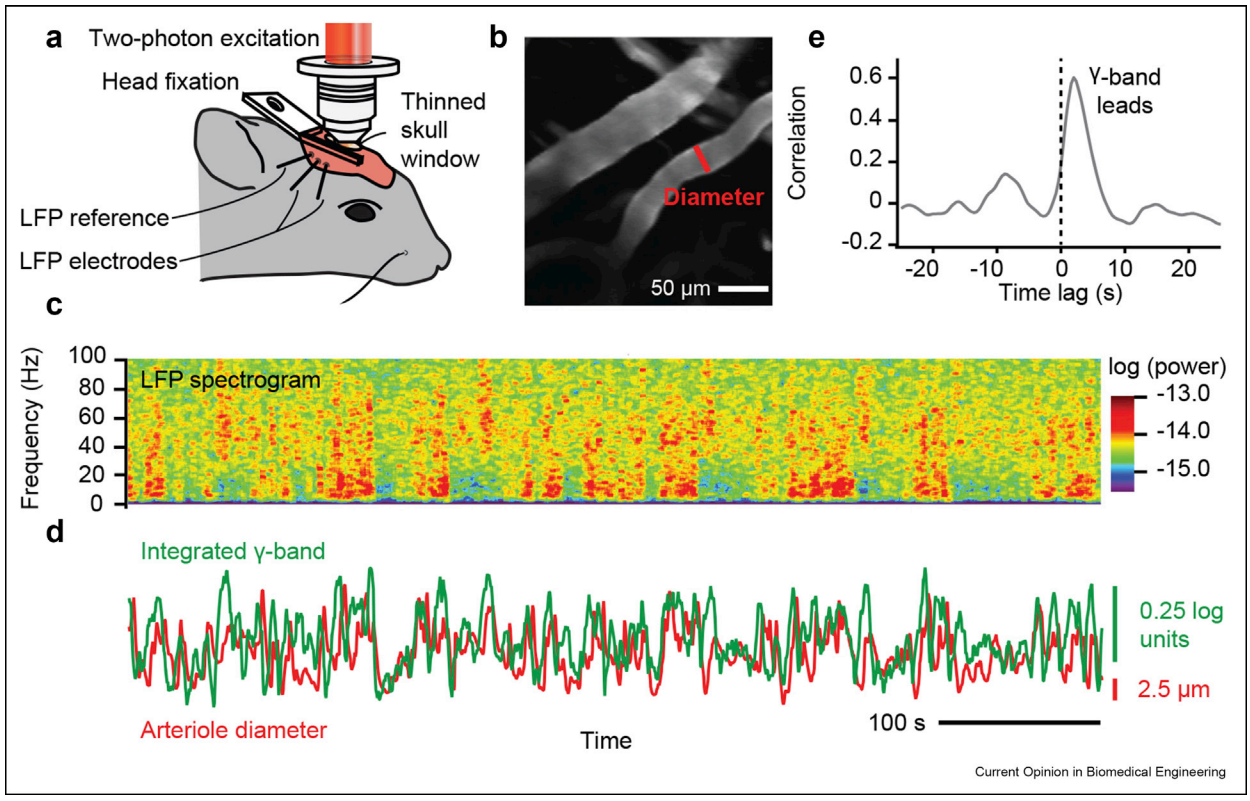

Coupling of γ oscillations and vasodilation in mouse cortex. (**a).** Setup with the head-fixed awake mouse. (**b).** Two-photon image of surface vessels. (**c).** Local field potential (LFP) spectrogram. (**d).** Overlaid time series of γ-band power and vessel diameter. (**e).** Cross correlation of the two time series; diameter lags by 1.9 s. For details, see Ref. [12].

neuromodulatory circuits coordinate neuronal and vascular/hemodynamic patterns of cortical activity in the context of *naturally occurring brain states*, as recently observed with brain-wide coexpression of optical probes for acetylcholine and neuronal intracellular Ca^{2+} [58]. These measurements can also be combined with another recent neurophotonics highlight: optically transparent surface electrode arrays [59–62]. These arrays offer simultaneous space-resolved LFP recordings to bridge novel optical readouts to the 'gold standard' electrophysiological measures of brain waves that have been traditionally used to characterize brain states [63,64].

The concept of the pial neurovascular circuit

A fundamental feature of cortical pial arterioles is that their diameter naturally oscillates at a frequency around 0.1 Hz as a consequence of intrinsic ionic properties of the vascular mural cells and propagation of dilation/constriction signaling along the vessel wall [65,66]. This signaling arrives from local cortical activity, subcortical nuclei, and neuromodulatory inputs (reviewed in Ref. [67]). The endothelial cells, which form the lumen of every vessel and interact through low resistance gap junctions to each other and to smooth muscle [68], play a key role in communication from neurons to arteriolar smooth muscle cells through retrograde electrical conduction along the capillary vessel wall [59]; therefore, conceptually one can think of a 'pial neurovascular circuit' that is composed of a network of pial arterioles that integrate different neuronal inputs to produce patterns of coherent oscillations in arteriolar diameter across the cortical mantle. These patterns contain regions that oscillate at slightly different frequencies [69]; that is, they parcellate into separate regions (Figure 2). The fascinating possibility is that these large-scale vascular/hemodynamic patterns may be invertible; that is, they may permit inference of brain state and regional aspects of neuronal processing with noninvasive measurement modalities such as fMRI applicable to humans.

As a means to address the potential inversion of large-scale vascular/hemodynamic patterns, future studies will leverage multimodal fluorescence imaging and fMRI in high-field animal scanners [70–73], using awake behaving mice with chronic optical windows [74,75], as a step towards human translation. With this technological progress, one can address how

Figure 2

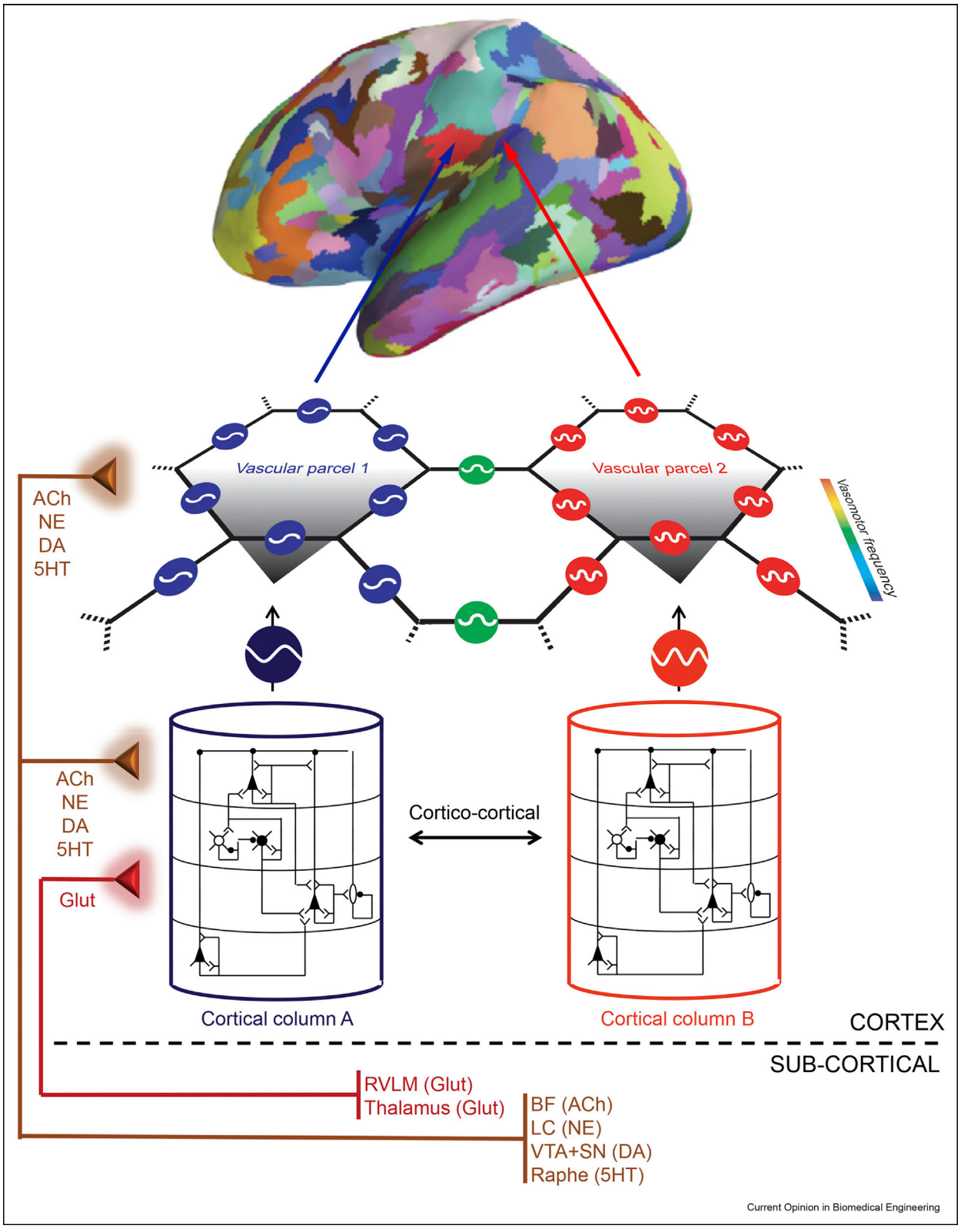

Conceptual model of the pial neurovascular circuit that drives parcellation of hemodynamics across the cortex. Parcels correspond to regions in which the BOLD signal oscillates as one but is asynchronous from neighboring regions. We hypothesize that these regions correspond to oscillations in the diameter of pial arterioles (drawn as a hexagonal array). BF – basal forebrain; LC – locus coeruleus; VTA – ventral tegmental area; SN –

Figure 3

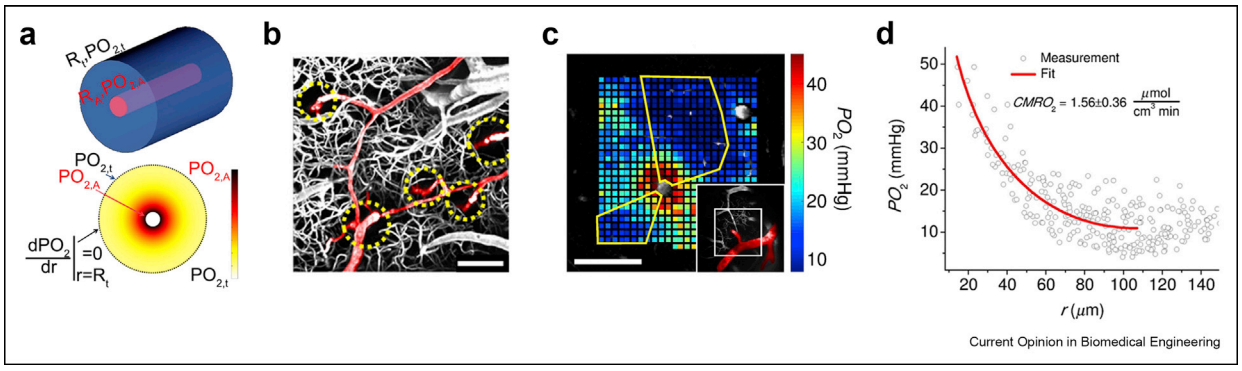

Two-photon imaging of pO_2 and estimation of $CMRO_2$. (**a**). Schematic illustration of the Krogh model parameters for extraction of $CMRO_2$. (**b**). Cortical vascular morphology approximating the model conditions. (**c**). Tissue pO_2 measurements; regions segmented for quantification are outlined in yellow. (**d**). Radial gradient of pO_2 around the diving arteriole in (c). For details see Ref. [82].

hemodynamic patterns can mimic the underlying neuronal activity characteristic of specific brain states and, further, with what reliability brain states be inferred from noninvasive fMRI readouts.

Neuromodulation and brain metabolism

Both cerebral blood flow and O_2 consumption contribute to fMRI signals

The BOLD signal reflects neuronal activity through its relationship with CBF and cerebral metabolic rate of O_2 ($CMRO_2$) [10,76]. Computational studies have attributed most of the net energetic cost of the brain to synaptic signaling [77]; therefore, the activity of neuromodulatory synapses acting onto both excitatory and inhibitory local cortical neurons is likely to increase $CMRO_2$; however, it has been proposed that neuromodulation may enhance the signal-to-noise ratio for salient stimuli by suppression of background neuronal activity, in part by altering the balance between local excitation and inhibition [44,78]. In agreement with this ansatz, a human positron emission tomography (PET) study has shown a decrease in glucose utilization within the default network [79], which is implicated in introspective states after administration of the monoamine transporter blocker methylphenidate (Ritalin) [80]. Thus, the question of the net metabolic cost of neuromodulation remains elusive, and this cost is likely to vary across different cortical regions.

Traditionally, estimation of $CMRO_2$ required two measurements related to blood flow and O_2 extraction (reviewed in Ref. [81]). Recently, Sakadzic et al. [82] introduced a new method for extraction of $CMRO_2$ that is based on a single imaging modality, that is, two-photon phosphorescence lifetime microscopy (2PLM), to provide measurements of the partial pressure of O_2 (pO_2) (Figure 3) (reviewed in Ref. [83]). The sensitivity of this method has been significantly improved by the arrival of a second-generation phosphorescent pO_2 nanoprobe [84]. Combining 2PLM with optical imaging of the release of neuromodulatory neurotransmitters [52] will help address the question of how $CMRO_2$ corresponds to different brain states. These measurements are also needed for bottom-up modeling of BOLD fMRI signals [85], as well as an estimate of energetic costs that are covered by nonoxidative metabolism.

Neuromodulation and aerobic glycolysis

The energetic costs of neuronal activity are reflected in the conversion of adenosine triphosphate (ATP) to adenosine diphosphate (ADP), and the ATP is restored through the oxidative metabolism of glucose. Glycolysis metabolizes glucose to pyruvate with the production of a small amount of ATP, and the pyruvate is subsequently shuttled to mitochondria for oxidative phosphorylation (OXPHOS) and the production of much more ATP, that is, about 15 times that of glycolysis. Under resting or unstimulated conditions, the cerebral metabolic rates of glucose (CMRglc) and $CMRO_2$ are well matched at 5.5:1 [86] nearly six O_2 per glucose, which corresponds to nearly complete oxidation of glucose [87]. Under stimulation, however, CMRglc increases more than $CMRO_2$; this suggests uncoupling between glycolysis and OXPHOS (reviewed in Ref. [88]). The phenomenon of glycolysis outstripping OXPHOS despite the availability of O_2 is called aerobic glycolysis (AG). Although excess glycolysis helps to provide additional

substantia nigra; ACh – acetylcholine; NE – norepinephrine; DA – dopamine; 5HT – serotonin; Glut – glutamate. The brain image is reproduced from Ref. [114].

ATP, this is a much less efficient route for ATP production than OXPHOS. During AG, the intermediate substrate pyruvate is converted to lactate, which is then transported into the extracellular space. Indeed, an increase in neuronal activity coincides with raising extracellular lactate [89,90] or even export of lactate from the brain under certain conditions [88]. All told, the occurrence of AG when O_2 appears to be available is puzzling. A recent thermodynamic analysis points to the need to maintain the O_2/CO_2 ratio in the mitochondria as a means to increase the pyruvate concentration [91]. Yet, from the perspective of imaging, AG does not consume O_2 and thus does not directly affect the BOLD signal.

On the cellular level, it has been proposed that AG preferentially occurs in astrocytes [92,93]. Further, it has been hypothesized that OXPHOS and AG are compartmentalized between neurons and astrocytes, such that astrocytes extract glucose from blood through the action of glucose transporters on astrocytic endfeet and break it down to lactate, which is secreted into the extracellular space. The extracellular lactate is then taken up by neurons and used as a substrate for neuronal OXPHOS. This so-called 'lactate shuttle' hypothesis [94] remains controversial. Experiments in cell cultures and brain slices have shown that both neurons and astrocytes are capable of shifting between the oxidative and glycolytic pathways depending on the experimental conditions [95,96]. *In vivo* mouse studies have not resolved this controversy, although some differences in their results could be attributed to anesthesia [97,98]. Of special note, a recent study with awake mice responding to a startle stimulus reported that lactate

Figure 4

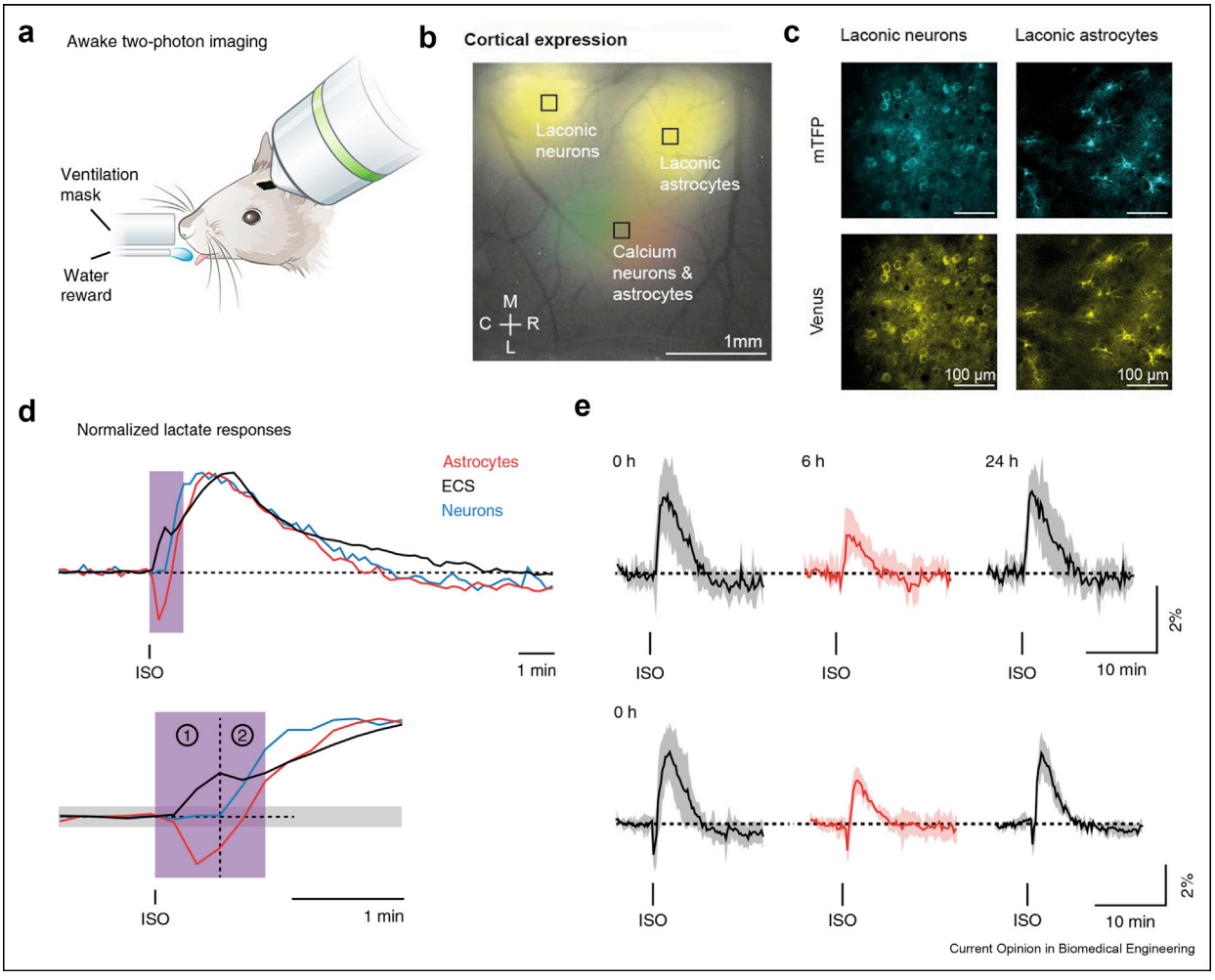

Lactate dynamics in cerebral neurons and astrocytes. (**a**). Setup with the head-fixed awake mouse. (**b**). Expression of genetically encoded probes for lactate (Laconic) and Ca^{2+} in the cerebral cortex. (**c**). High-resolution images of Laconic expression in cerebral neurons and astrocytes. (**d**). Time-course of lactate changes in neurons, astrocytes, and the extracellular space (ECS) in response to a sniff of isoflurane (ISO). (e). Inhibition of β-adrenergic receptors reduces the evoked response in neurons (top) and astrocytes (bottom). For details, see Ref. [98].

transients in neurons and astrocytes were reduced by blocking β-adrenergic signaling (Figure 4) and that these cellular lactate surges were impaired in transgenic mice lacking the ability to store glycogen in the brain [98]. These findings are in line with prior literature on adrenergic control of glycolysis and glycogenolysis (reviewed in Refs. [88,99]), suggesting that the relative contribution of OXPHOS and AG to the energy metabolism in the cerebral cortex, as well as the metabolic partnership between cerebral neurons and astrocytes, may be dependent on brain state.

A number of targetable genetically encoded optical probes for cellular metabolism have been recently developed, including those for lactate and pyruvate [100], glucose [95], nicotinamide adenine dinucleotide (NADH) [101], and adenosine triphosphate (ATP) [102]. Nevertheless, microscopic measurements of CMRglc currently remain beyond reach. This inability follows from the need to account for the rates of metabolic reactions rather than measure the instantaneous concentrations of metabolites [88]. A probe of extracellular concentration of secreted metabolites, such as lactate, would be a welcome addition to neurovascular research.

Aerobic glycolysis and aging

The brain has a relatively high metabolic rate during development that gradually decreases with maturation and aging. A meta-analysis of human PET studies has concluded that AG peaks in young, 3- to 5-yr-old, children [103], although it remains unclear whether consumption of glucose in excess of oxygen by developing brains should be attributed to the support of neuronal activity, biosynthesis, or both [88,103,104]. Interestingly, the immature cortex often exhibits an 'inverted' hemodynamic response, represented by a weaker blood flow increase compared to the $CMRO_2$ increase prior to maturation of neurovascular coupling mechanisms [105]. Upregulation of AG could partly offset the need for increased $CMRO_2$ for increased ATP production and help prevent a sustained oxygenation drop during brain states with a high level of metabolism, such as the rapid eye movement (REM) sleep [106,107].

Glucose metabolism, oxygen consumption, and cerebral blood flow all decrease in the aging brain [108]. Human PET studies that concurrently measured O_2 and glucose consumption have shown that age-related decreases in brain glycolysis exceed the decrease in oxygen consumption, which results in selective loss of AG [103,104]. In parallel, a number of recent human neuroimaging studies on aging have demonstrated a weakening of cortical oscillations, including those in the γ-band [109,110]. This suggests a decline in neuromodulatory neurotransmission, although decreased tissue volume in aging can also modulate these signals. A decrease in γ-band activity was also observed in a recent study of Jessen et al. [111] in aged mice, paralleled by a 2-fold increase in stimulus-induced $CMRO_2$. These studies, taken together, suggest that age-dependent dysregulation of neuromodulatory signaling could underlie the deficit in AG that leads to an increase in OXPHOS to sustain metabolic loads. The increase in OXPHOS may, in turn, lead to oxidative stress and mitochondrial dysfunction that is a hallmark of aging [112].

Understanding the relative contribution of OXPHOS and AG in brain maturation and aging, along with regulation of the respective pathways by neuromodulation, will lead to insights into brain energetics and age-specific metabolic departures. In mice, we now can start to address these issues using longitudinal optical imaging of neuromodulators and metabolites and concurrent electrophysiological recordings with optically transparent electrode arrays.

Conclusions

We have highlighted several recent neurophotonic advances that offer a novel, unprecedented view on cell-type-specific and brain-state-specific mechanisms that drive and modulate brain metabolism and fMRI signals. Of particular interest is the ability to understand the phenomena of parcellation of the ∼0.1 Hz vasomotor oscillations in BOLD fMRI. This provides a basis to identify separate regions in the human [69] and mouse [113] brain and is used to define default networks [79]. The high spatial and temporal resolution of neurophotonic tools, in combination with the lower resolution but brain-wide imaging capability of MRI, is a potent combination to delineate the biophysics of fMRI in terms of brain activation and brain state. These efforts provide a path to at least probabilistically solve the inverse problem of deducing brain state, as well as aspects of neuronal computation, from de novo BOLD fMRI images.

Declaration of competing interest

The authors declare that they have no known competing financial interests or personal relationships that could have appeared to influence the work reported in this paper.

Acknowledgements

We thank Gerry Dienel for the valuable discussions. We gratefully acknowledge support from the NIH (BRAIN Initiative R01MH111359, BRAIN Initiative R01MH111438, R01DA050159, R35NS097265).

References

Papers of particular interest, published within the period of review, have been highlighted as:

* of special interest
** of outstanding interest

1. Stringer C, Pachitariu M, Steinmetz N, Reddy CB, Carandini M, Harris KD: **Spontaneous behaviors drive multidimensional, brainwide activity**. *Science* 2019, **364**:255.

2. Frostig RD, Xiong Y, Chen-Bee CH, Kvasnak E, Stehberg J: **Large-scale organization of rat sensorimotor cortex based on a motif of large activation spreads**. *J Neurosci* 2008, **28**: 13274–13284.

3. McIlwain JT: **Receptive fields of optic tract axons and lateral geniculate cells: peripheral extent and barbiturate sensitivity**. *J Neurophysiol* 1964, **27**:1154–1173.

4. ** Leopold DA, Maier A: **Ongoing physiological processes in the cerebral cortex**. *Neuroimage* 2012, **62**:2190–2200.
Reviews the electrophysiological studies on linking neural activity to ongoing fMRI fluctuations.

5. ** Smith SM, Fox PT, Miller KL, Glahn DC, Fox PM, Mackay CE, Filippini N, Watkins KE, Toro R, Laird AR, *et al.*: **Correspondence of the brain's functional architecture during activation and rest**. *Proc Natl Acad Sci U S A* 2009, **106**: 13040–13045.
Primary demonstration of the consistency of networks determined from multiple targeted activation tasks and resting-state networks identified without using any tasks.

6. ** Glasser MF, Coalson TS, Robinson EC, Hacker CD, Harwell J, Yacoub E, Ugurbil K, Andersson J, Beckmann CF, Jenkinson M, *et al.*: **A multi-modal parcellation of human cerebral cortex**. *Nature* 2016, **536**:171–178.
Parcellation of the cortical surface into 180 areas based on data from the Human Connectome Project (HCP). The parcellation algorithm was based on differences in cortical architecture, function, connectivity, and/or topography.

7. * Eickhoff SB, Yeo BTT, Genon S: **Imaging-based parcellations of the human brain**. *Nat Rev Neurosci* 2018, **19**:672–686.
Reviews the different approaches for defining distinct partitions of the brain based on anatomical areas or networks of interacting regions.

8. Gutierrez-Barragan D, Basson MA, Panzeri S, Gozzi A: **Infra-slow state fluctuations govern spontaneous fMRI network dynamics**. *Curr Biol* 2019, **29**:2295–2306. e2295.

9. Devor A, Boas D, Einevoll GT, Buxton RB, Dale AM: **Neuronal basis of non-invasive functional imaging: from microscopic neurovascular dynamics to BOLD fMRI**. In Choi RG In-Young. *Neural metabolism in vivo*, vol. 4. Springer; 2012.

10. ** Uhlirova H, Kilic K, Tian P, Sakadzic S, Gagnon L, Thunemann M, Desjardins M, Saisan PA, Nizar K, Yaseen MA, *et al.*: **The roadmap for estimation of cell-type-specific neuronal activity from non-invasive measurements**. *Philos Trans R Soc Lond B Biol Sci* 2016:371.
Outlines the roadmap for leveraging mechanistic insights from animal studies to accurately draw physiological inferences from noninvasive signals in humans.

11. Mitra A, Kraft A, Wright P, Acland B, Snyder AZ, Rosenthal Z, Czerniewski L, Bauer A, Snyder L, Culver J, *et al.*: **Spontaneous infra-slow brain activity has unique spatiotemporal dynamics and laminar structure**. *Neuron* 2018, **98**:297–305. e296.

12. ** Mateo C, Knutsen PM, Tsai PS, Shih AY, Kleinfeld D: **Entrainment of arteriole vasomotor fluctuations by neural activity is a basis of blood-oxygenation-level-dependent "Resting-State" connectivity**. *Neuron* 2017, **96**:936–948. e933.
Using optical imaging methods, this study showed that ultra-slow frequency (~0.1 Hz) fluctuations in the γ-band power entrain the dynamics of arteriolar vasomotion coupling the slowly varying amplitude of the ongoing rhythm to the resting-state fMRI signal.

13. ** Ma Y, Shaik MA, Kozberg MG, Kim SH, Portes JP, Timerman D, Hillman EM: **Resting-state hemodynamics are spatiotemporally coupled to synchronized and symmetric neural activity in excitatory neurons**. *Proc Natl Acad Sci U S A* 2016, **113**: E8463–E8471.
Primary demonstration in mice that ongoing fluctuations in local blood volume are coupled to underlying patterns of excitatory neuronal activity.

14. Wright PW, Brier LM, Bauer AQ, Baxter GA, Kraft AW, Reisman MD, Bice AR, Snyder AZ, Lee JM, Culver JP: **Functional connectivity structure of cortical calcium dynamics in anesthetized and awake mice**. *PloS One* 2017, **12**, e0185759.

15. Matsui T, Murakami T, Ohki K: **Transient neuronal coactivations embedded in globally propagating waves underlie resting-state functional connectivity**. *Proc Natl Acad Sci U S A* 2016, **113**:6556–6561.

16. * He Y, Wang M, Chen X, Pohmann R, Polimeni JR, Scheffler K, Rosen BR, Kleinfeld D, Yu X: **Ultra-slow single-vessel BOLD and CBV-based fMRI spatiotemporal dynamics and their correlation with neuronal intracellular calcium signals**. *Neuron* 2018, **97**:925–939. e925.
The authors performed simultaneous single-vessel fMRI and neuronal Ca^{2+} measurements using fiber photometry. They reported a 2-mm correlation length, which bears on the resolution of functional connectivity.

17. He BJ, Snyder AZ, Zempel JM, Smyth MD, Raichle ME: **Electrophysiological correlates of the brain's intrinsic large-scale functional architecture**. *Proc Natl Acad Sci U S A* 2008, **105**: 16039–16044.

18. Brookes MJ, Woolrich M, Luckhoo H, Price D, Hale JR, Stephenson MC, Barnes GR, Smith SM, Morris PG: **Investigating the electrophysiological basis of resting state networks using magnetoencephalography**. *Proc Natl Acad Sci U S A* 2011, **108**:16783–16788.

19. Kucyi A, Schrouff J, Bickel S, Foster BL, Shine JM, Parvizi J: **Intracranial electrophysiology reveals reproducible intrinsic functional connectivity within human brain networks**. *J Neurosci* 2018, **38**:4230–4242.

20. Hacker CD, Snyder AZ, Pahwa M, Corbetta M, Leuthardt EC: **Frequency-specific electrophysiologic correlates of resting state fMRI networks**. *Neuroimage* 2017, **149**:446–457.

21. Aedo-Jury F, Schwalm M, Hamzehpour L, Stroh A: **Brain states govern the spatio-temporal dynamics of resting-state functional connectivity**. *Elife* 2020, **9**.

22. * Jaime S, Gu H, Sadacca BF, Stein EA, Cavazos JE, Yang Y, Lu H: **Delta rhythm orchestrates the neural activity underlying the resting state BOLD signal via phase-amplitude coupling**. *Cerebr Cortex* 2019, **29**:119–133.
Simultaneous fMRI and LFP recording reveal distinct correlations of the fMRI signal with the LFP power within specific spectral bands.

23. ** Wang M, He Y, Sejnowski TJ, Yu X: **Brain-state dependent astrocytic Ca(2+) signals are coupled to both positive and negative BOLD-fMRI signals**. *Proc Natl Acad Sci U S A* 2018, **115**:E1647–E1656.
The authors performed simultaneous whole-brain fMRI and Ca^{2+} measurements in cortical astrocytes using fiber photometry. The study showed that astrocytic activity depended on activation of the thalamus and midbrain reticular formation bearing on a potential brain-state dependency of neurovascular coupling.

24. Wen H, Liu Z: **Broadband electrophysiological dynamics contribute to global resting-state fMRI signal**. *J Neurosci* 2016, **36**:6030–6040.

25. Wu TL, Yang PF, Wang F, Shi Z, Mishra A, Wu R, Chen LM, Gore JC: **Intrinsic functional architecture of the non-human primate spinal cord derived from fMRI and electrophysiology**. *Nat Commun* 2019, **10**:1416.

26. Schwalm M, Schmid F, Wachsmuth L, Backhaus H, Kronfeld A, Aedo Jury F, Prouvot PH, Fois C, Albers F, van Alst T, *et al.*: **Cortex-wide BOLD fMRI activity reflects locally-recorded slow oscillation-associated calcium waves**. *Elife* 2017, **6**.

27. Tsai PS, Mateo C, Field JJ, Schaffer CB, Anderson ME, Kleinfeld D: **Ultra-large field-of-view two-photon microscopy**. *Optic Express* 2015, **23**:13833–13847.

28. Sofroniew NJ, Flickinger D, King J, Svoboda K: **A large field of view two-photon mesoscope with subcellular resolution for in vivo imaging**. *Elife* 2016, **5**.

29. Stirman JN, Smith IT, Kudenov MW, Smith SL: **Wide field-of-view, multi-region, two-photon imaging of neuronal activity in the mammalian brain**. *Nat Biotechnol* 2016, **34**:857–862.

30. Lecoq J, Savall J, Vucinic D, Grewe BF, Kim H, Li JZ, Kitch LJ, Schnitzer MJ: **Visualizing mammalian brain area interactions by dual-axis two-photon calcium imaging**. *Nat Neurosci* 2014, **17**:1825–1829.

31. Vanni MP, Chan AW, Balbi M, Silasi G, Murphy TH: **Mesoscale mapping of mouse cortex reveals frequency-dependent cycling between distinct macroscale functional modules**. *J Neurosci* 2017, **37**:7513–7533.

32. Shih AY, Mateo C, Drew PJ, Tsai PS, Kleinfeld D: **A polished and reinforced thinned-skull window for long-term imaging of the mouse brain**. *J Vis Exp* 2012.

33. Kim TH, Zhang Y, Lecoq J, Jung JC, Li J, Zeng H, Niell CM, Schnitzer MJ: **Long-Term optical access to an estimated one million neurons in the live mouse cortex**. *Cell Rep* 2016, **17**: 3385–3394.

34. Dana H, Mohar B, Sun Y, Narayan S, Gordus A, Hasseman JP, Tsegaye G, Holt GT, Hu A, Walpita D, *et al.*: **Sensitive red protein calcium indicators for imaging neural activity**. *Elife* 2016, **5**.

35. Adachi Y, Osada T, Sporns O, Watanabe T, Matsui T, Miyamoto K, Miyashita Y: **Functional connectivity between anatomically unconnected areas is shaped by collective network-level effects in the macaque cortex**. *Cerebr Cortex* 2012, **22**:1586–1592.

36. * Shine JM, van den Brink RL, Hernaus D, Nieuwenhuis S, Poldrack RA: **Catecholaminergic manipulation alters dynamic network topology across cognitive states**. *Netw Neurosci* 2018, **2**:381–396.

This paper identified a low-dimensional manifold of fMRI dynamics across cognitive tasks and found that these dimensions were coupled to neuromodulatory receptor architecture. These results linked fMRI spatiotemporal dynamics with neurotransmitter maps within the human brain.

37. Klaassens BL, Rombouts SA, Winkler AM, van Gorsel HC, van der Grond J, van Gerven JM: **Time related effects on functional brain connectivity after serotonergic and cholinergic neuromodulation**. *Hum Brain Mapp* 2017, **38**:308–325.

38. van den Brink RL, Pfeffer T, Donner TH: **Brainstem modulation of large-scale intrinsic cortical activity correlations**. *Front Hum Neurosci* 2019, **13**:340.

39. ** Turchi J, Chang C, Ye FQ, Russ BE, Yu DK, Cortes CR, Monosov IE, Duyn JH, Leopold DA: **The basal forebrain regulates global resting-state fMRI fluctuations**. *Neuron* 2018, **97**: 940–952. e944.

This study showed that pharmacological inactivation of cholinergic projections from the nucleus basalis Meynert affects resting-state fMRI signals within the affected hemisphere.

40. Chandler DJ, Jensen P, McCall JG, Pickering AE, Schwarz LA, Totah NK: **Redefining noradrenergic neuromodulation of behavior: impacts of a modular locus coeruleus architecture**. *J Neurosci* 2019, **39**:8239–8249.

41. Zerbi V, Floriou-Servou A, Markicevic M, Vermeiren Y, Sturman O, Privitera M, von Ziegler L, Ferrari KD, Weber B, De Deyn PP, *et al.*: **Rapid reconfiguration of the functional connectome after chemogenetic locus coeruleus activation**. *Neuron* 2019, **103**:702–718. e705.

42. * Ferenczi EA, Zalocusky KA, Liston C, Grosenick L, Warden MR, Amatya D, Katovich K, Mehta H, Patenaude B, Ramakrishnan C, *et al.*: **Prefrontal cortical regulation of brainwide circuit dynamics and reward-related behavior**. *Science* 2016, **351**, aac9698.

These author combined fMRI with OG stimulation of the VTA and the medial prefrontal cortex (mPFC) in awake rats to study brain-wide circuits mediating the dopaminergic regulation of reward-seeking behavior.

43. Wang D, Wang X, Liu P, Jing S, Du H, Zhang L, Jia F, Li A: **Serotonergic afferents from the dorsal raphe decrease the excitability of pyramidal neurons in the anterior piriform cortex**. *Proc Natl Acad Sci U S A* 2020, **117**:3239–3247.

44. Thiele A, Bellgrove MA: **Neuromodulation of attention**. *Neuron* 2018, **97**:769–785.

45. Shine JM, Breakspear M, Bell PT, Ehgoetz Martens KA, Shine R, Koyejo O, Sporns O, Poldrack RA: **Human cognition involves the dynamic integration of neural activity and neuromodulatory systems**. *Nat Neurosci* 2019, **22**:289–296.

46. * Turner KL, Gheres KW, Proctor EA, Drew PJ: **Neurovascular coupling and bilateral connectivity during NREM and REM sleep**. *Elife* 2020, **9**.

This study measured neuronal and hemodynamic signals across wakefulness, NREM, and REM sleep and observed profound modulation of neurovascular coupling dependent on brain state. Importantly, they found that sleep is common in head-fixed animals, so state-dependent neurovascular dynamics may be a common component of signals measured in many systems neuroscience experiments.

47. Hamel E: **Perivascular nerves and the regulation of cerebrovascular tone**. *J Appl Physiol* 2006, **100**:1059–1064 (1985).

48. Choi JK, Chen YI, Hamel E, Jenkins BG: **Brain hemodynamic changes mediated by dopamine receptors: role of the cerebral microvasculature in dopamine-mediated neurovascular coupling**. *Neuroimage* 2006, **30**:700–712.

49. Cardin JA: **Snapshots of the brain in action: local circuit operations through the lens of gamma oscillations**. *J Neurosci* 2016, **36**:10496–10504.

50. McGinley MJ, David SV, McCormick DA: **Cortical membrane potential signature of optimal states for sensory signal detection**. *Neuron* 2015, **87**:179–192.

51. von Engelhardt J, Eliava M, Meyer AH, Rozov A, Monyer H: **Functional characterization of intrinsic cholinergic interneurons in the cortex**. *J Neurosci* 2007, **27**:5633–5642.

52. Sabatini BL, Tian L: **Imaging neurotransmitter and neuromodulator dynamics in vivo with genetically encoded indicators**. *Neuron* 2020, **108**:17–32.

53. Nguyen QT, Schroeder LF, Mank M, Muller A, Taylor P, Griesbeck O, Kleinfeld D: **An in vivo biosensor for neurotransmitter release and in situ receptor activity**. *Nat Neurosci* 2010, **13**:127–132.

54. Jing M, Zhang P, Wang G, Feng J, Mesik L, Zeng J, Jiang H, Wang S, Looby JC, Guagliardo NA, *et al.*: **A genetically encoded fluorescent acetylcholine indicator for in vitro and in vivo studies**. *Nat Biotechnol* 2018, **36**:726–737.

55. Muller A, Joseph V, Slesinger PA, Kleinfeld D: **Cell-based reporters reveal in vivo dynamics of dopamine and norepinephrine release in murine cortex**. *Nat Methods* 2014, **11**: 1245–1252.

56. Patriarchi T, Cho JR, Merten K, Howe MW, Marley A, Xiong WH, Folk RW, Broussard GJ, Liang R, Jang MJ, *et al.*: **Ultrafast neuronal imaging of dopamine dynamics with designed genetically encoded sensors**. *Science* 2018:360.

57. Wan J, Peng W, Li X, Qian T, Song K, Zeng J, Deng F, Hao S, Feng J, Zhang P, *et al.*: *A genetically encoded GRAB sensor for measuring serotonin dynamics in vivo*. bioArxiv; 2020.

58. ** Lohani S, Moberly AH, Benisty H, Landa B, Jing M, Li Y, Higley MJ, Cardin JA: *Dual color mesoscopic imaging reveals spatiotemporally heterogeneous coordination of cholinergic and neocortical activity*. bioRxiv; 2020. 2020.12.09.418632.

These author combined large-scale imaging of cortical acetylcholine release with imaging of neuronal Ca^{2+} activity in awake mice to study the relationship between the behavioral state, dynamics of local cortical circuits, and cholinergic modulation.

59. Lu Y, Liu X, Hattori R, Ren C, Zhang X, K T, Kuzum D: **Ultralow impedance graphene microelectrodes with high optical transparency for simultaneous deep two-photon imaging in transgenic mice**. *Adv Funct Mater* 2018, **28**.

60. Thunemann M, Lu Y, Liu X, Kilic K, Desjardins M, Vandenberghe M, Sadegh S, Saisan PA, Cheng Q, Weldy KL, *et al.*: **Deep 2-photon imaging and artifact-free optogenetics through transparent graphene microelectrode arrays**. *Nat Commun* 2018, **9**:2035.

61. Hossain L, Thunemann M, Devor A, Dayeh SA: **Chronic 2-photon calcium imaging through transparent PEDOT:PSS microelectrode arrays in awake mice**. In *Optical Society of America*. Fort Lauderdale: OSA; 2020.

62. Renz AF, Lee J, Tybrandt K, Brzezinski M, Lorenzo DA, Cheraka MC, Lee J, Helmchen F, Vörös J, Lewis CM: *Opto-E-dura: a soft, stretchable ECoG array for multimodal, multi-scale neuroscience*. bioRxiv; 2020.

63. Poulet JFA, Crochet S: **The cortical states of wakefulness**. *Front Syst Neurosci* 2018, **12**:64.

64. Brown EN, Lydic R, Schiff ND: **General anesthesia, sleep, and coma**. *N Engl J Med* 2010, **363**:2638–2650.

65. Longden TA, Dabertrand F, Koide M, Gonzales AL, Tykocki NR, Brayden JE, Hill-Eubanks D, Nelson MT: **Capillary K^+-sensing initiates retrograde hyperpolarization to increase local cerebral blood flow**. *Nat Neurosci* 2017, **20**:717–726.

66. Rungta RL, Chaigneau E, Osmanski BF, Charpak S: **Vascular compartmentalization of functional hyperemia from the synapse to the pia**. *Neuron* 2018, **99**:362–375 e364.

67. * Drew PJ, Mateo C, Turner KL, Yu X, Kleinfeld D: **Ultra-slow oscillations in fMRI and resting-state connectivity: neuronal and vascular contributions and technical confounds**. *Neuron* 2020, **107**:782–804.
A detailed perspective and review of how resting-state correlations may arise from entrainment of intrinsic slow variation of arteriolar diameter by the slow variation of the envelope of high frequency (gamma) neuronal activity.

68. Welsh DG, Tran CHT, Hald BO, Sancho M: **The conducted vasomotor response: function, biophysical basis, and pharmacological control**. *Annu Rev Pharmacol Toxicol* 2018, **58**:391–410.

69. Mitra PP, Ogawa S, Hu X, Ugurbil K: **The nature of spatiotemporal changes in cerebral hemodynamics as manifested in functional magnetic resonance imaging**. *Magn Reson Med* 1997, **37**:511–518.

70. Chen Y, Pais-Roldan P, Chen X, Frosz MH, Yu X: **MRI-guided robotic arm drives optogenetic fMRI with concurrent Ca(2+) recording**. *Nat Commun* 2019, **10**:2536.

71. Schulz K, Sydekum E, Krueppel R, Engelbrecht CJ, Schlegel F, Schroter A, Rudin M, Helmchen F: **Simultaneous BOLD fMRI and fiber-optic calcium recording in rat neocortex**. *Nat Methods* 2012, **9**:597–602.

72. * Lake EMR, Ge X, Shen X, Herman P, Hyder F, Cardin JA, Higley MJ, Scheinost D, Papademetris X, Crair MC, *et al.*: **Simultaneous cortex-wide fluorescence Ca(2+) imaging and whole-brain fMRI**. *Nat Methods* 2020.
Combination of resting-state fMRI with simultaneous large-scale Ca^{2+} imaging.

73. * Pais-Roldán P, Takahashi K, Sobczak F, Chen Y, Zhao X, Zeng H, Jiang Y, Yu X: **Indexing brain state-dependent pupil dynamics with simultaneous fMRI and optical fiber calcium recording**. *Proc Natl Acad Sci U S A* 2020, **117**:6875–6882.
This study performed simultaneous pupilometry, resting-state fMRI, and Ca^{2+} imaging in anesthetized rats. It identified a focal correlate of pupil diameter within noradrenergic nuclei and demonstrated its link to the spectral dynamics of the calcium signal.

74. * Desjardins M, Kilic K, Thunemann M, Mateo C, Holland D, Ferri CGL, Cremonesi JA, Li B, Cheng Q, Weldy KL, *et al.*: **Awake mouse imaging: from two-photon microscopy to blood oxygen level-dependent functional magnetic resonance imaging**. *Biol Psychiatry Cogn Neurosci Neuroimaging* 2019, **4**:533–542.
This study demonstrated BOLD fMRI in awake mice with implanted glass cranial windows used for optical imaging and/or OG manipulations.

75. Fonseca MS, Bergomi MG, Mainen ZF, Shemesh N: *Functional MRI of large scale activity in behaving mice*. bioRxiv; 2020.

76. Buxton RB, Griffeth VE, Simon AB, Moradi F, Shmuel A: **Variability of the coupling of blood flow and oxygen metabolism responses in the brain: a problem for interpreting BOLD studies but potentially a new window on the underlying neural activity**. *Front Neurosci* 2014, **8**:139.

77. * Hall CN, Klein-Flugge MC, Howarth C, Attwell D: **Oxidative phosphorylation, not glycolysis, powers presynaptic and postsynaptic mechanisms underlying brain information processing**. *J Neurosci* 2012, **32**:8940–8951.
Study supporting the view that the major mechanisms mediating brain information processing are all initially powered by oxidative phosphorylation, and an astrocyte–neuron lactate shuttle is not needed for this to occur.

78. Koob GF, Volkow ND: **Neurobiology of addiction: a neurocircuitry analysis**. *Lancet Psychiatry* 2016, **3**:760–773.

79. Raichle ME, MacLeod AM, Snyder AZ, Powers WJ, Gusnard DA, Shulman GL: **A default mode of brain function**. *Proc Natl Acad Sci U S A* 2001, **98**:676–682.

80. Volkow ND, Fowler JS, Wang GJ, Telang F, Logan J, Wong C, Ma J, Pradhan K, Benveniste H, Swanson JM: **Methylphenidate decreased the amount of glucose needed by the brain to perform a cognitive task**. *PloS One* 2008, **3**, e2017.

81. Gagnon L, Smith AF, Boas DA, Devor A, Secomb TW, Sakadzic S: **Modeling of cerebral oxygen transport based on in vivo microscopic imaging of microvascular network structure, blood flow, and oxygenation**. *Front Comput Neurosci* 2016, **10**:82.

82. Sakadzic S, Yaseen MA, Jaswal R, Roussakis E, Dale AM, Buxton RB, Vinogradov SA, Boas DA, Devor A: **Two-photon microscopy measurement of cerebral metabolic rate of oxygen using periarteriolar oxygen concentration gradients**. *Neurophotonics* 2016, **3**, 045005.

83. Devor A, Sakadzic S, Yaseen MA, Roussakis E, Tian P, Slovin H, Vanzetta I, Teng IC, Saisan PA, Sinks LE, *et al.*: **Functional imaging of cerebral oxygenation with intrinsic optical contrast and phosphorescent probes**. In *Optical imaging of cortical circuit dynamics*. Edited by Weber B, Helmchen F, Springer; 2013.

84. Esipova TV, Barrett MJP, Erlebach E, Masunov AE, Weber B, Vinogradov SA: **Oxyphor 2P: a high-performance probe for deep-tissue longitudinal oxygen imaging**. *Cell Metabol* 2019.

85. ** Gagnon L, Sakadzic S, Lesage F, Musacchia JJ, Lefebvre J, Fang Q, Yucel MA, Evans KC, Mandeville ET, Cohen-Adad J, *et al.*: **Quantifying the microvascular origin of BOLD-fMRI from first principles with two-photon microscopy and an oxygen-sensitive nanoprobe**. *J Neurosci* 2015, **35**:3663–3675.
A bottom-up computation of BOLD fMRI signals using experimentally obtained microscopic parameters.

86. Mergenthaler P, Lindauer U, Dienel GA, Meisel A: **Sugar for the brain: the role of glucose in physiological and pathological brain function**. *Trends Neurosci* 2013, **36**:587–597.

87. Hyder F, Fulbright RK, Shulman RG, Rothman DL: **Glutamatergic function in the resting awake human brain is supported by uniformly high oxidative energy**. *J Cerebr Blood Flow Metabol* 2013, **33**:339–347.

88. Dienel GA: **Brain glucose metabolism: integration of energetics with function**. *Physiol Rev* 2019, **99**:949–1045.

89. Mazuel L, Blanc J, Repond C, Bouchaud V, Raffard G, Deglon N, Bonvento G, Pellerin L, Bouzier-Sore AK: **A neuronal MCT2 knockdown in the rat somatosensory cortex reduces both the NMR lactate signal and the BOLD response during whisker stimulation**. *PloS One* 2017, **12**, e0174990.

90. Li B, Freeman RD: **Neurometabolic coupling between neural activity, glucose, and lactate in activated visual cortex**. *J Neurochem* 2015, **135**:742–754.

91. ** Buxton RB: **The thermodynamics of thinking: connections between neural activity, energy metabolism and blood flow**. *Philos Trans R Soc Lond B Biol Sci* 2021, **376**:20190624.
Describes the hypothesis that the larger changes of blood flow and glucose metabolism compared to oxygen metabolism may be a physiological mechanism to preserve the entropy change available from OXPHOS that powers the production of ATP, and thus, help prevent a fall in the phosphorylation potential.

92. Magistretti PJ, Pellerin L, Rothman DL, Shulman RG: **Energy on demand**. *Science* 1999, **283**:496–497.

93. Kasischke KA, Vishwasrao HD, Fisher PJ, Zipfel WR, Webb WW: **Neural activity triggers neuronal oxidative metabolism followed by astrocytic glycolysis**. *Science* 2004, **305**:99–103.

94. Pellerin L, Magistretti PJ: **Sweet sixteen for ANLS**. *J Cerebr Blood Flow Metabol* 2012, **32**:1152–1166.

95. Diaz-Garcia CM, Yellen G: **Neurons rely on glucose rather than astrocytic lactate during stimulation**. *J Neurosci Res* 2019, **97**:883–889.

96. Yellen G: **Fueling thought: management of glycolysis and oxidative phosphorylation in neuronal metabolism**. *J Cell Biol* 2018, **217**:2235–2246.

97. Diaz-Garcia CM, Mongeon R, Lahmann C, Koveal D, Zucker H, Yellen G: **Neuronal stimulation triggers neuronal glycolysis and not lactate uptake**. *Cell Metabol* 2017, **26**:361–374. e364.

98. ** Zuend M, Saab AS, Wyss MT, Ferrari KD, Hösli L, Looser ZJ, Stobart JL, Duran J, Guinovart JJ, Barros LF, *et al.*: **Arousal-induced cortical activity triggers lactate release from astrocyt**. *Nature Metabolism* 2020, **2**:179–191.
A two-photon imaging study in awake mice showing that arousal-evoked cellular lactate surges depend on intact β-adrenergic signaling and functional glycogen stores.

99. Dienel GA, Cruz NF: **Aerobic glycolysis during brain activation: adrenergic regulation and influence of norepinephrine on astrocytic metabolism**. *J Neurochem* 2016, **138**:14–52.

100. Machler P, Wyss MT, Elsayed M, Stobart J, Gutierrez R, von Faber-Castell A, Kaelin V, Zuend M, San Martin A, Romero-Gomez I, *et al.*: **In vivo evidence for a lactate gradient from astrocytes to neurons**. *Cell Metabol* 2016, **23**:94–102.

101. Hung YP, Yellen G: **Live-cell imaging of cytosolic NADH-NAD+ redox state using a genetically encoded fluorescent biosensor**. *Methods Mol Biol* 2014, **1071**:83–95.

102. Lobas MA, Tao R, Nagai J, Kronschlager MT, Borden PM, Marvin JS, Looger LL, Khakh BS: **A genetically encoded single-wavelength sensor for imaging cytosolic and cell surface ATP**. *Nat Commun* 2019, **10**:711.

103. Goyal MS, Hawrylycz M, Miller JA, Snyder AZ, Raichle ME: **Aerobic glycolysis in the human brain is associated with development and neotenous gene expression**. *Cell Metabol* 2014, **19**:49–57.

104. * Goyal MS, Vlassenko AG, Blazey TM, Su Y, Couture LE, Durbin TJ, Bateman RJ, Benzinger TL, Morris JC, Raichle ME: **Loss of brain aerobic glycolysis in normal human aging**. *Cell Metabol* 2017, **26**:353–360. e353.
A meta-analysis of published human PET studies that measured CMRO2 and CMRGlc, showing selective reduction of AG during development and aging.

105. Kozberg MG, Chen BR, DeLeo SE, Bouchard MB, Hillman EM: **Resolving the transition from negative to positive blood oxygen level-dependent responses in the developing brain**. *Proc Natl Acad Sci U S A* 2013, **110**:4380–4385.

106. Townsend RE, Prinz PN, Obrist WD: **Human cerebral blood flow during sleep and waking**. *J Appl Physiol* 1973, **35**: 620–625.

107. Braun AR, Balkin TJ, Wesenten NJ, Carson RE, Varga M, Baldwin P, Selbie S, Belenky G, Herscovitch P: **Regional cerebral blood flow throughout the sleep-wake cycle. An H2(15)O PET study**. *Brain* 1997, **120**(Pt 7):1173–1197.

108. Mattson MP, Arumugam TV: **Hallmarks of brain aging: adaptive and pathological modification by metabolic states**. *Cell Metabol* 2018, **27**:1176–1199.

109. Murty D, Manikandan K, Kumar WS, Ramesh RG, Purokayastha S, Javali M, Rao NP, Ray S: **Gamma oscillations weaken with age in healthy elderly in human EEG**. *Neuroimage* 2020, **215**:116826.

110. ElShafei HA, Fornoni L, Masson R, Bertrand O, Bidet-Caulet A: **Age-related modulations of alpha and gamma brain activities underlying anticipation and distraction**. *PloS One* 2020, **15**, e0229334.

111. Jessen SB, Mathiesen C, Lind BL, Lauritzen M: **Interneuron deficit associates attenuated network synchronization to mismatch of energy supply and demand in aging mouse brains**. *Cerebr Cortex* 2017, **27**:646–659.

112. Dai DF, Chiao YA, Marcinek DJ, Szeto HH, Rabinovitch PS: **Mitochondrial oxidative stress in aging and healthspan**. *Longev Heal* 2014, **3**:6.

113. Chan AW, Mohajerani MH, LeDue JM, Wang YT, Murphy TH: **Mesoscale infraslow spontaneous membrane potential fluctuations recapitulate high-frequency activity cortical motifs**. *Nat Commun* 2015, **6**:7738.

114. Blumensath T, Jbabdi S, Glasser MF, Van Essen DC, Ugurbil K, Behrens TEJ, Smith SM: **Spatially constrained hierarchical parcellation of the brain with resting-state fMRI**. *Neuroimage* 2013, **76**:313–324.